

# Effects of Nb<sub>2</sub>O<sub>5</sub> addition on the sinterability, microstructure and mechanical behaviour of ZTM-Al<sub>2</sub>O<sub>3</sub>

X.H. Jin<sup>a</sup>, L. Gao<sup>a,\*</sup>, Y.R. Chen<sup>b</sup>, Q.M. Yuan<sup>b</sup>

<sup>a</sup>State Key Lab. of High Performance Ceramics and Superfine Microstructures, Shanghai Institute of Ceramics, 1295 Dingxi Road, Shanghai, 200050, PR China

<sup>b</sup>School of Material Science, Tianjin University, 300072, PR China

Received 27 November 1999; received in revised form 8 April 2000; accepted 8 April 2000

## Abstract

ZTM–Al<sub>2</sub>O<sub>3</sub> ceramics doped with Y<sub>2</sub>O<sub>3</sub>, MgO and Nb<sub>2</sub>O<sub>5</sub> were studied. These ceramics could achieve high density at a sintering temperature as low as 1390°C. Results showed that there was a critical Nb<sub>2</sub>O<sub>5</sub>/ZrO<sub>2</sub> weight ratio. When Nb<sub>2</sub>O<sub>5</sub>/ZrO<sub>2</sub> was lower than the critical value, Nb<sub>2</sub>O<sub>5</sub> addition had little influence on the sintering, otherwise the sinterability could be considerably improved. The microstructure of all the samples were homogenous; no obvious difference in microstructure had been brought about by Nb<sub>2</sub>O<sub>5</sub>. Despite this, X-ray diffraction measurement showed a continuous increase in m-ZrO<sub>2</sub> with Nb<sub>2</sub>O<sub>5</sub>, due to a deficiency of oxygen vacancy in ZrO<sub>2</sub>. As a result, the mechanical properties of the ceramics, especially toughness, were greatly improved, because of the enhancement of microcrack toughening mechanism by m-ZrO<sub>2</sub>. © 2000 Elsevier Science Ltd. All rights reserved.

*Keywords:* Mullite; Nb<sub>2</sub>O<sub>5</sub>; Toughening; Sinterability; ZrO<sub>2</sub>; ZTM–Al<sub>2</sub>O<sub>3</sub>

## 1. Introduction

Mullite is recognized as one of the most promising engineering materials for applications at elevated temperature due to its excellent chemical stability, good creep resistance and low thermal expansion. However, its ambient temperature properties are poor, which gives a serious drawback to its utilization. In order to combat the inherent weakness of the material, many reinforcing agents, e.g. dispersed rigid particulate, fibers (whiskers) and ZrO<sub>2</sub>, are incorporated, producing composites of much superior properties by utilizing the additive or even synergistic effects of many toughening mechanisms.<sup>1–6</sup> Composites making use of multi-toughening by the addition of ZrO<sub>2</sub> and SiC whisker were examined by Clausen and Petzow.<sup>1</sup> They measured the toughness of pure mullite, 10 vol.% ZrO<sub>2</sub>-mullite, 20 vol.% SiC whisker-mullite and 20 vol.% SiC whisker-10 vol.% ZrO<sub>2</sub>-mullite as 2.8, 3.5, 4.4, and 5.4 MPa m<sup>0.5</sup>, respectively. The bending strengths were 244–452 and 580 MPa, respectively. A considerable multi-toughening is achieved by addition of ZrO<sub>2</sub> and SiC whisker. Yang

Z.F.<sup>2</sup> Hong J.S.<sup>3</sup>, Becher<sup>4</sup> and Ruh<sup>5</sup> also reported similar favorable results. Finally, Guo<sup>6</sup> used SiC particulate and ZrO<sub>2</sub> to reinforce mullite. He found that the two reinforcing agents had an additive effect on the toughness of mullite. However, SiC is prone to oxidation at high temperature. SiC whisker is expensive and harmful for human health. These limit the scope of application of the materials. In our experiment, Al<sub>2</sub>O<sub>3</sub> was selected as the rigid dispersoid because of its high elastic modulus, good high temperature stability and good chemical compatibility with mullite. In order to lower the sintering temperature and, at the same time, to adjust the phase assemblage in the ceramics, MgO, Y<sub>2</sub>O<sub>3</sub> and Nb<sub>2</sub>O<sub>5</sub> were added. In this paper, we mainly study the effects of Nb<sub>2</sub>O<sub>5</sub> on the sintering and mechanical properties of the ZrO<sub>2</sub>-toughened-mullite–Al<sub>2</sub>O<sub>3</sub> (ZTM–Al<sub>2</sub>O<sub>3</sub>) ceramics.

## 2. Experimental procedure

Industrial grade ZrO<sub>2</sub>, Al<sub>2</sub>O<sub>3</sub>, fused mullite and other additives of analysis grade purity were used as starting materials. They were mixed together by a ball-milling process, using 3Y-TZP grinding medium in distilled water. After drying and calcining, the powder obtained was uniaxially pressed into compacts of Ø50×10 mm

\* Corresponding author. Tel.: +86-216-251-2990, ext 6321; fax: +86-216-2513903.

E-mail address: liangaoc@online.sh.cn (L. Gao).

dimension, then isostatically cold-pressed at 200 MPa. Sintering was conducted pressurelessly in open air. The sintered ceramic discs were ground with a diamond wheel and cut into  $5 \times 2.5 \times 40$  mm<sup>3</sup> rectangular bars for mechanical property measurement. Bulk density was tested by a water displacement method. X-ray diffraction (XRD) was carried out on a diffractometer using Ni-filtered Cu-K $\alpha$  radiation for phase identification. The initial compositions of all the ceramics include 47 wt.% mullite, 32 wt.% ZrO<sub>2</sub>, 21 wt.% Al<sub>2</sub>O<sub>3</sub>, 1.8 wt.% Y<sub>2</sub>O<sub>3</sub>, 0.2 wt.% MgO and 0.0 to 1.4 wt.% of Nb<sub>2</sub>O<sub>5</sub>. The content of Nb<sub>2</sub>O<sub>5</sub> increases in an interval of 0.35wt.%, the corresponding samples are defined as A1 to A5 in ascending order (Table 1).

### 3. Results and discussion

#### 3.1. Sinterability of ZTM–Al<sub>2</sub>O<sub>3</sub>

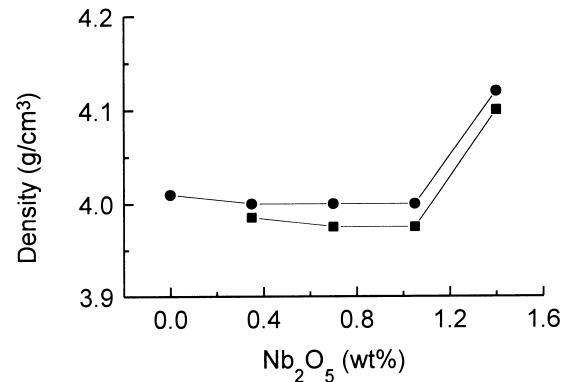
For mullite ceramics, the addition of alkaline earth oxide and/or rare earth oxide usually introduces a liquid phase in the ceramics, which considerably enhances the densification process.<sup>7–9</sup> Regarding the effects of rare metal oxide, there are few reports. Fig. 1(A) shows the bulk density of ZTM–Al<sub>2</sub>O<sub>3</sub> as a function of Nb<sub>2</sub>O<sub>5</sub> (rare metal oxide) content. There is a critical Nb<sub>2</sub>O<sub>5</sub> value. Nb<sub>2</sub>O<sub>5</sub> less than 1.05 wt.% has little effect on the bulk density of the ceramics; however, the latter rises abruptly when Nb<sub>2</sub>O<sub>5</sub> content exceeds this value. In fact, we have found a similar feature in a ZTM (ZrO<sub>2</sub>-toughened-mullite) ceramics prepared by us in a parallel experiment. The composition of the ZTM consists of 24.2 wt.% ZrO<sub>2</sub>, 75.8 wt.% mullite, 2.3 wt.% Y<sub>2</sub>O<sub>3</sub> and various amounts of Nb<sub>2</sub>O<sub>5</sub>. In this case, the critical value of Nb<sub>2</sub>O<sub>5</sub> content is 0.9 wt.% [see Fig. 1(B)]. However, what is interesting is that, in both cases, the critical weight ratios of Nb<sub>2</sub>O<sub>5</sub> to ZrO<sub>2</sub> in these ceramics are all approximately equal to 0.035. This implies that the behaviour of Nb<sub>2</sub>O<sub>5</sub> in promoting the sintering of mullite must be affected by the presence of ZrO<sub>2</sub>.

The solution of Nb<sub>2</sub>O<sub>5</sub> in ZrO<sub>2</sub> has been unambiguously verified,<sup>10</sup> so it is reasonable to assume that when Nb<sub>2</sub>O<sub>5</sub> content is low, Nb<sub>2</sub>O<sub>5</sub> may preferably be incorporated into ZrO<sub>2</sub> to form solid solution rather than entering the liquid phase, hence its promoting effect on the sintering of the ceramics is offset. When Nb<sub>2</sub>O<sub>5</sub> content exceeds a

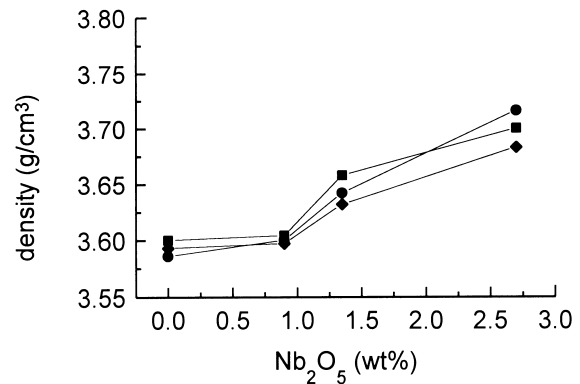
certain critical value (e.g. 1.05 wt.% in ZTM–Al<sub>2</sub>O<sub>3</sub>), a larger proportion of Nb<sub>2</sub>O<sub>5</sub> enters the liquid phase, which considerably enhances sintering.

#### 3.2. Phase assemblage and microstructure

In order to clarify the changes that Nb<sub>2</sub>O<sub>5</sub> has brought to the ZTM–Al<sub>2</sub>O<sub>3</sub> ceramics, XRD was conducted on



(A) ZTM–Al<sub>2</sub>O<sub>3</sub> (circle:1420°C; square:1390°C)



(B) ZTM (circle:1520°C; square:1540°C; diamond: 1560°C)

Fig. 1. Densities of ZTM(-Al<sub>2</sub>O<sub>3</sub>) as a function of Nb<sub>2</sub>O<sub>5</sub> content.

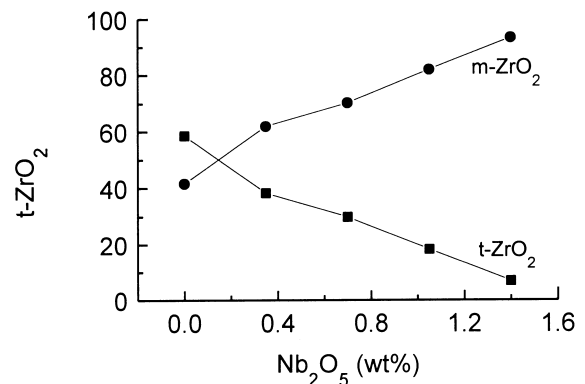


Fig. 2. (m,t)-ZrO<sub>2</sub> content as a function of Nb<sub>2</sub>O<sub>5</sub> addition.

Table 1  
Chemical compositions and serial numbers of ZTM–Al<sub>2</sub>O<sub>3</sub> samples (wt.%)

	Mullite	ZrO <sub>2</sub>	Al <sub>2</sub> O <sub>3</sub>	Y <sub>2</sub> O <sub>3</sub>	MgO	Nb <sub>2</sub> O <sub>5</sub>
A1	47	32	21	1.8	0.2	0.0
A2	47	32	21	1.8	0.2	0.35
A3	47	32	21	1.8	0.2	0.4
A4	47	32	21	1.8	0.2	1.05
A5	47	32	21	1.8	0.2	1.4

the samples sintered at 1420°C for 2 h. No other new phases existing in them were detected, except the already expected (t,m)-ZrO<sub>2</sub>, mullite and Al<sub>2</sub>O<sub>3</sub>. However, the relative contents of t-ZrO<sub>2</sub> and m-ZrO<sub>2</sub> have changed, with the former decreasing and the latter increasing with Nb<sub>2</sub>O<sub>5</sub> addition (Fig. 2). The authors ascribe the phenomenon to the more severe deficiency in oxygen vacancy in ZrO<sub>2</sub> with increasing Nb<sub>2</sub>O<sub>5</sub> addition, which lowers the stability of the high temperature polymorphs of ZrO<sub>2</sub>.<sup>10</sup>

Fig. 3 presents the scanning electron microscope (SEM) micrographs of the thermally etched A1, A3 and A5 samples. The bright spherical particles are ZrO<sub>2</sub>, other grey equiaxed ones are mullite and Al<sub>2</sub>O<sub>3</sub>. (Because the atomic numbers of Si and Al are very close, it is difficult to distinguish between Al<sub>2</sub>O<sub>3</sub> and mullite in a secondary electron image.) Compared with mullite or Al<sub>2</sub>O<sub>3</sub>, ZrO<sub>2</sub> particles are smaller in size and most of them are located at grain boundaries, only a few very tiny ZrO<sub>2</sub> have

entered mullite/Al<sub>2</sub>O<sub>3</sub> grains. These intragranular ZrO<sub>2</sub> particles engulfed by growing mullite/Al<sub>2</sub>O<sub>3</sub> grains are much smaller than intergranular ones and take a nearly perfect sphere geometry in order to minimize the energy of the composite microsystem.

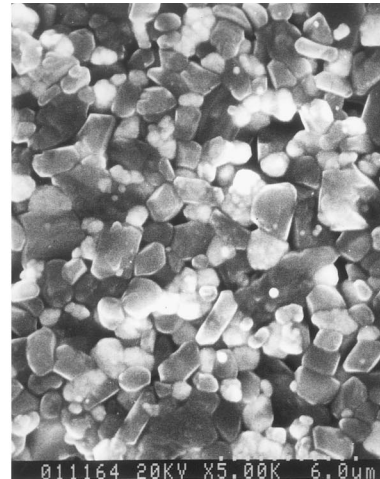
In general, the microstructure of all these samples are relatively dense and homogeneous; there are essentially no obvious differences between them, no accelerated grain growth has occurred with increasing Nb<sub>2</sub>O<sub>5</sub> doping. This suggests that Nb<sub>2</sub>O<sub>5</sub> is a desirable additive, it does not accelerate the grain growth in the ceramics, although effective in promoting sintering.

### 3.3. Mechanical performances and toughening mechanisms

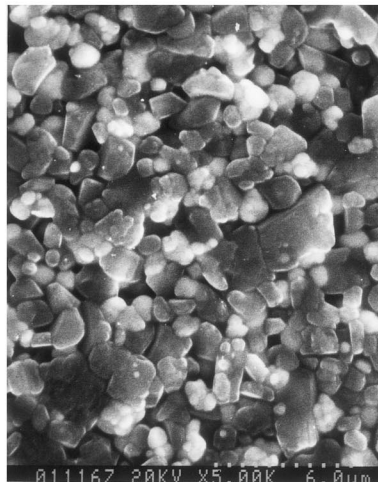
Plots of mechanical properties versus Nb<sub>2</sub>O<sub>5</sub> content are illustrated in Fig. 4. The toughness of the samples



(A) A1



(B) A3



(C) A5

Fig. 3. SEM micrographs of ZTM–Al<sub>2</sub>O<sub>3</sub>.

sintered at 1390 and 1420°C increase with Nb<sub>2</sub>O<sub>5</sub>, while the strengths rise to their maximum values at first then decline with Nb<sub>2</sub>O<sub>5</sub>.

According to the theories of fracture mechanics, for a brittle material such as ceramics the square of its fracture toughness ( $K_{IC}$ ) can be expressed by the following equation.<sup>11</sup>

$$K_{IC}^2 = 2E\gamma \quad (1)$$

where  $E$  and  $\gamma$  are the elastic modulus and fracture energy of the material. Supposing that  $\gamma_0$  and  $K_0$  correspond to the  $\gamma$  and  $K_{IC}$  values of a crack-free ceramics;

$\Delta\gamma$  and  $\Delta K_{IC}^2$  are the increases in  $\gamma$  and  $K_{IC}^2$  of a microcracked ceramics relative to a crack-free one. Then the following formula exists:

$$\begin{cases} \gamma = \gamma_0 + \Delta\gamma \\ K_{IC}^2 = K_0^2 + \Delta K_{IC}^2 \end{cases} \quad (2)$$

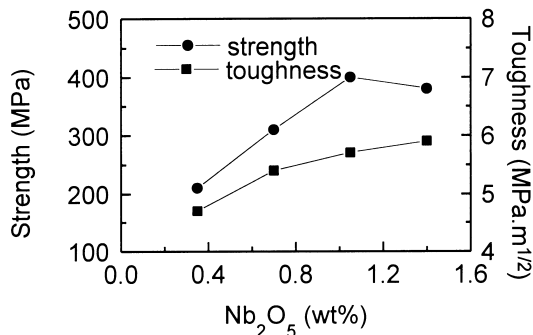
Substitute (2) into (1):

$$\Delta K_{IC}^2 = 2E\Delta\gamma \quad (3)$$

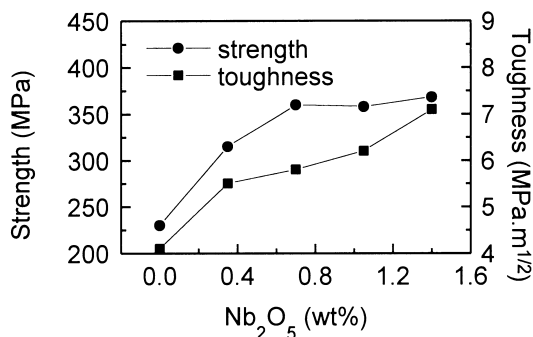
Rice<sup>12</sup> argued that in a microcrack-toughened ceramics the upper limits of  $\Delta\gamma$  could be expressed as:

$$\Delta\gamma = \frac{2\pi a \gamma_{mc} V_f L}{d} \quad (4)$$

where  $L$  and  $a$  are the long and short axes of the microcracked process zone;  $d$  and  $V_f$  are the diameter and volume fraction of the microcrack initiating second phase particulate;  $\gamma_{mc}$  is the microcrack interfacial fracture energy. Supposing that microcracks in ZTM–Al<sub>2</sub>O<sub>3</sub> are mainly induced by m-ZrO<sub>2</sub>, i.e.  $V_f = V_m$ , for microcrack toughened ZTM–Al<sub>2</sub>O<sub>3</sub>,  $K_{IC}^2$  should be proportional to the volume fraction of m-ZrO<sub>2</sub> ( $V_m$ ). Fig. 5 clarifies the relationship between  $K_{IC}^2$  and  $V_m$  in a ZTM–Al<sub>2</sub>O<sub>3</sub> ceramics sintered at 1420°C.  $K_{IC}^2$  increases linearly with m-ZrO<sub>2</sub>



(A) sintered at 1390°C



(B) sintered at 1420°C

Fig. 4. Mechanical properties of ZTM–Al<sub>2</sub>O<sub>3</sub> as a function of Nb<sub>2</sub>O<sub>5</sub> content.

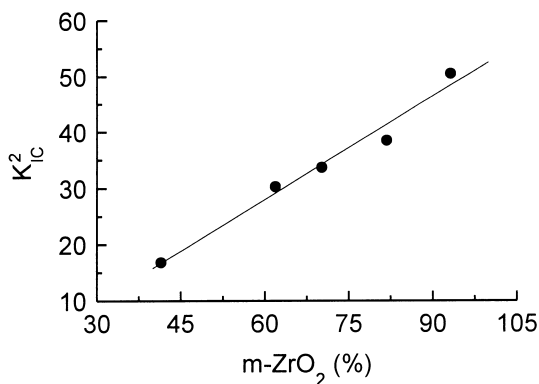
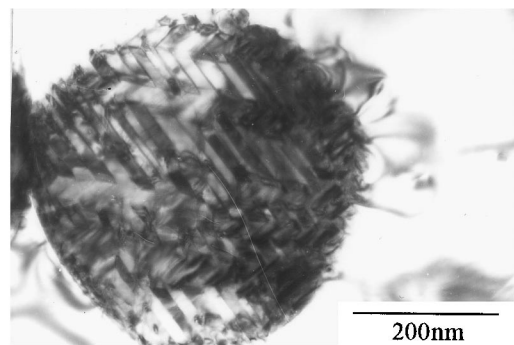
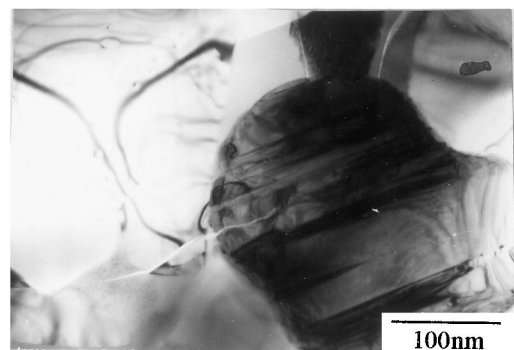


Fig. 5. Relationship between  $K_{IC}^2$  and m-ZrO<sub>2</sub> content.



(A) stress field near a m-ZrO<sub>2</sub> particle



(B) radial microcracks around a m-ZrO<sub>2</sub> particle

Fig. 6. TEM images showing the stress field and radial microcracks around m-ZrO<sub>2</sub> particles.

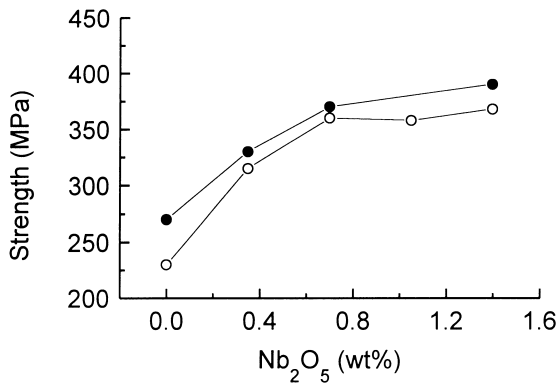


Fig. 7. Ambient temperature (open circle) and 800°C (solid circle) strength of ZTM–Al<sub>2</sub>O<sub>3</sub> as a function of Nb<sub>2</sub>O<sub>5</sub> content.

content, which is consistent with the above prediction. Therefore, microcrack toughening should be one of the most important toughening mechanisms operating in the ceramics. And since the remarkable decrease in t-ZrO<sub>2</sub> content does not lead to deterioration to the toughness, stress induced phase transformation toughening should occupy a relatively less important position.

The existence of local stress field and microcracks around m-ZrO<sub>2</sub> is verified by the transmission electron microscope (TEM) micrographs in Fig. 6. In Fig. 6(A), the large spherical particle is m-ZrO<sub>2</sub>, which can be determined from its twined structure. In the vicinity of the m-ZrO<sub>2</sub> particle, there are stress fringes resulting from the volume expansion associated with t-ZrO<sub>2</sub>–m-ZrO<sub>2</sub> transformation. Fig. 6(B) shows the microcracks initiated by local stress around a m-ZrO<sub>2</sub>. Because the tangential stress is a tensile one, all cracks radiate from the center of the m-ZrO<sub>2</sub>. These microcracks and stress field around m-ZrO<sub>2</sub> will surely induce crack deflection and bifurcation, which can remarkably increase the energy consumption of a propagating crack. As a result, the toughness of the ceramics is improved. Fig. 7 presents the strengths of ZTM–Al<sub>2</sub>O<sub>3</sub> ceramics at room temperature and 800°C versus Nb<sub>2</sub>O<sub>5</sub> content. As can be seen, the strengths at 800°C are all relatively higher than their counterparts at room temperature. If stress induced phase transformation is the dominant toughening mechanism, the strength will decrease when the testing temperature is raised to 800°C because of the absence of the stress induced transformation of t-ZrO<sub>2</sub> particles. This also suggests that phase transformation toughening is not the major toughening mechanism in ZTM–Al<sub>2</sub>O<sub>3</sub>. The strength increase at 800°C probably results from softening of the glass phase at the grain boundary, because the plastic deformation of the softened glass phase can reduce stress concentration near the crack tip and increase the energy needed for crack propagation.

In Fig. 4, the m-ZrO<sub>2</sub> content in the ceramics will increase with Nb<sub>2</sub>O<sub>5</sub>; therefore, the improvement in mechanical properties is brought about by m-ZrO<sub>2</sub> enhanced microcrack toughening. The decrease in strength at a high Nb<sub>2</sub>O<sub>5</sub> regime is the consequence of microcrack interlinking because of the high microcrack concentration in the ceramics, which seriously limits the strength of the material.

#### 4. Conclusion

Now, we have discussed the influence of Nb<sub>2</sub>O<sub>5</sub> addition on a variety of characteristics of ZTM–Al<sub>2</sub>O<sub>3</sub>. In summary, Nb<sub>2</sub>O<sub>5</sub> is helpful for the sintering of the ceramics, if Nb<sub>2</sub>O<sub>5</sub> content is greater than 1.05 wt.%. At the same time, Nb<sub>2</sub>O<sub>5</sub> addition has led to the change in the relative content of m-ZrO<sub>2</sub> and t-ZrO<sub>2</sub>, with the former increasing and the latter decreasing with Nb<sub>2</sub>O<sub>5</sub>. As a result, the mechanical properties of the ceramics are notably improved, due to an enhanced microcrack toughening.

#### References

1. Claussen, N., Whisker-reinforced oxide ceramics. *J. Phys.*, 1986, **47**, 693–702.
2. Yang, Z. F., Xu, H. Y., Tan, J. Q. and Yuan, Q. M., Mechanical properties of mullite-based composites. *J. Chin. Ceram. Soc.*, 1989, **17**, 467–472.
3. Hong, J. S., Huang, X. X., Guo, J. K. and Li, B. S., Mechanical properties and microstructure of SiC<sub>w</sub>-mullite and SiC<sub>w</sub>-Y-TZP-mullite composites. *J. Chin. Ceram. Soc.*, 1992, **20**, 410–416.
4. Becher, P. F. and Tiegs, T. W., Toughening behavior involving multiple mechanism: whisker reinforcement and zirconia toughening. *J. Am. Ceram. Soc.*, 1987, **70**, 651–654.
5. Ruh, R. and Mazdiyashi, K. S., Mechanical and microstructural characterisation of mullite and mullite-SiC whisker and ZrO<sub>2</sub>-toughened-mullite-SiC-whisker composite. *J. Am. Ceram. Soc.*, 1988, **71**, 503–512.
6. Guo, J. K., The progress and application prospect of structural ceramics in china. *J. Chin. Ceram. Soc. Bull.*, 1995, **14**(4), 18–28.
7. Fang, D. Y. and Hwang, C. S., Effects of Y<sub>2</sub>O<sub>3</sub> addition on the sinterability and microstructure of mullite (part 2): crystallization of liquid phase and grain growth. *J. Ceram. Soc. Jpn.*, 1993, **101**, 331–335.
8. Mitamura, T., Kobayashi, H., Ishibashi, N. and Akiba, T., Effects of rare earth oxide addition on the sintering of mullite. *J. Ceram. Soc. Jpn.*, 1991, **99**, 351–356.
9. Ushifusa, N. and Ogihara, S., Study of mullite III-a oxide ceramics. *J. Ceram. Soc. Jpn.*, 1989, **97**, 690–698.
10. Jin, X. H., Ding, X. and Chen, Y. R., Influences of pentavalent oxides Nb<sub>2</sub>O<sub>5</sub> and Ta<sub>2</sub>O<sub>5</sub> on the microstructure and properties of Y-TZP. *J. Chin. Ceram. Soc. Bull.*, 1999, **18**(2), 52–57.
11. Guan, Z. D., *Physical Properties of Inorganic Materials*. Qinghua, Beijing, 1995.
12. Rice, R. W., Is there anything of practical value hidden amongst the composite-toughening theories? *Ceram. Eng. Sci. Proc.*, 1990, **11**, 551–561.